Environmental
Science
Water Research & Technology

ROYAL SOCIETY
OF CHEMISTRY

PAPER

View Article Online
View Journal | View Issue

Cite this: *Environ. Sci.: Water Res. Technol.*, 2020, **6**, 383

Nutrient recovery from treated wastewater by a hybrid electrochemical sequence integrating bipolar membrane electrodialysis and membrane capacitive deionization†

Fei Gao,‡[abc] Li Wang, ‡[a] Jie Wang,[b] Hongwei Zhang[b] and Shihong Lin *[ad]

Received 4th November 2019,
Accepted 18th December 2019

DOI: 10.1039/c9ew00981g

rsc.li/es-water

The growing needs for sustainable nutrient management and pollution control have motivated the development of novel technologies for nutrient recovery from wastewater. However, most of the existing technologies require extensive use of chemicals and intensive consumption of energy to achieve substantial recovery of nutrients. Herein, we present a hybrid electrochemical sequence integrating two relatively novel electrochemical processes, bipolar membrane electrodialysis (BMED) and membrane capacitive deionization (MCDI), for simultaneous removal of phosphorus and nitrogen. Specifically, the BMED process is employed to alkalify the wastewater to facilitate struvite precipitation and the MCDI process is used to further reduce the ammonia concentration in the effluent and concentrate the excess ammonia to a small stream. The electrochemical sequence is demonstrated to remove ~89% of phosphorus and ~77% of ammonia, recovering ~81% of wastewater as a high-quality effluent that can be discharged or reused. This electrochemical treatment train minimizes chemical use and has competitive energy consumption as compared to electrochemical processes for nutrient recovery from wastewater.

Water impact

Removing nutrients from wastewater is very much needed for reducing the ecological impact of discharge and managing the nutrient cycle. But achieving it sustainably requires minimal use of chemicals and energy. Herein we demonstrate a hybrid electrochemical sequence with minimum chemical use and reasonable energy consumption as a possible way for effective nutrient removal and recovery from wastewater.

1. Introduction

Phosphorus and nitrogen are essential nutrients for agriculture. Phosphorus, as one of the most essential resources in society, is currently extracted from non-renewable phosphate reserve and is thus unsustainable.[1–3] It has been suggested that affordable phosphate reserve will be depleted in the foreseeable future unless there is a paradigm-shift in the way we manage phosphorus as a resource.[3–5] Meanwhile, excessive amounts of phosphorus and nitrogen in wastewater need to be removed to protect aquatic ecosystems from eutrophication and to meet growingly stringent discharge regulations.[6–11] To address these challenges, a new paradigm is needed for recovering valuable resources, especially nutrients, from wastewater. The sustainable and cost-effective removal and recovery of PO_4^{3-}–P and NH_4^+–N from municipal wastewater is of great research interest and societal importance.

A notable process that has been heavily investigated in recent years for resource recovery from wastewater is struvite ($MgNH_4PO_4{\cdot}6H_2O$) precipitation. In this process, both phosphorus and ammonium can be removed and recovered in the form of struvite precipitate which can be used as a slow-release fertilizer.[4,12,13] Precipitation of struvite is sensitive to pH and requires the pH to maintained above 8.5 (ref. 14 and 15) or even 9.0 when the treated wastewater has a low phosphate–P concentration (*e.g.*, lower than 1 mM).[16] Therefore, the addition of a base is always required to achieve the desired pH. In addition, NH_4^+–N in typical treated

---

[a] *Department of Civil and Environmental Engineering, Vanderbilt University, Nashville, Tennessee 37235-1831, USA. E-mail: shihong.lin@vanderbilt.edu; Tel: +1 615 322 7226*

[b] *State Key Laboratory of Separation Membranes and Membrane Processes, Tianjin Polytechnic University, Tianjin 300387, China*

[c] *School of Environmental Science and Engineering, Tianjin University, Tianjin 300072, China*

[d] *Department of Chemical and Biomolecular Engineering, Vanderbilt University, Nashville, Tennessee 37235-1604, USA*

† Electronic supplementary information (ESI) available. See DOI: 10.1039/c9ew00981g

‡ These authors contributed equally.

wastewater is stoichiometrically overabundant as compared to PO_4^{3-}–P. Therefore, struvite precipitation alone cannot effectively recover all the PO_4^{3-}–P and NH_4^+–N from the treated wastewater. Additional processes are required to further recover and remove the excess NH_4^+–N before the treated wastewater can be discharged.

The motivation behind this study is to develop a treatment train fully based on electrochemical processes to effectively achieve a high degree of PO_4^{3-}–P and NH_4^+–N recovery with minimum use of chemicals. The vision of achieving water and wastewater treatment with minimum or even no chemical use is based on the fact that the production of chemicals often creates additional environmental footprint and the transportation of chemicals also adds to logistics cost and challenges especially for treatment systems that are distributed and remote. In order to achieve the stated goal, we developed a hybrid electrochemical sequence combining bipolar membrane electrodialysis (BMED) for adjusting the pH for struvite precipitation and membrane capacitive deionization (MCDI) for recovering ammonium. A recent study demonstrates the simultaneous recovery of nitrogen and phosphorus using concurrent flow electrode capacitive deionization (FCDI).[17] This single-stage process focuses on nutrient removal from the treated water instead of recovering nutrients as a fertilizer.

Bipolar membrane electrodialysis (BMED) is a relatively novel electrodialysis technology that takes advantage of the special properties of a bipolar membrane for splitting water into protons (H^+) and hydroxide ions (OH^-) using an applied voltage.[18,19] BMED has been explored for generating acidic and alkaline solutions from various electrolytes.[20–22] It has also been integrated with different treatment processes to construct hybrid treatment trains where pH adjustment is required.[23,24] For example, it has been coupled with a microbial fuel cell (MFC) to produce an alkaline solution for biogas upgrading.[23] It has also been used to acidify seawater for extracting CO_2 from the dissolved carbonate system.[25] Not only can the use of BMED for pH adjustment eliminate the use of chemicals, it can also achieve precise control of pH by varying the current and the hydraulic residence time.

The other electrochemical unit process employed in this treatment train is membrane capacitive deionization (MCDI) which has been shown to be effective in separating charged ions from relatively dilute feed water.[26–29] MCDI, or some other variants of capacitive deionization based on activated carbon (AC), such as flow-electrode capacitive deionization,[30] removes charged ions from water *via* formation of an electrical double layer in the micropores of the AC electrodes. MCDI can be used to recover NH_4^+–N by removing NH_4^+ from a relatively large volume of the feed water, temporarily storing the NH_4^+ ions in the AC electrodes, and later releasing them to a relatively small volume of water as the concentrate rich in NH_4^+–N. In this way, the majority of the feed water has a sufficiently low concentration of NH_4^+–N for discharge or beneficial reuse, whereas the brine has a sufficiently high concentration of NH_4^+–N that can be applied as a fertilizer.

In this work, we demonstrate a hybrid treatment train integrating BMED, struvite precipitation, and multi-stage MCDI for the recovery of phosphorus and ammonium from wastewater. We first investigate the impact of operation parameters in BMED on its performance, and demonstrate that BMED can indeed increase the pH of the wastewater in the alkaline chamber to the desired level for struvite precipitation, while using simulated seawater in the acidic chamber to complete the setup. We then perform a three-stage MCDI process to further remove ammonium from the supernatant of the wastewater after struvite precipitation and generate a concentrate of ammonium. Finally, the overall performance of the treatment train was assessed in terms of removal efficiency, product water recovery, and energy consumption.

2. Materials and methods

2.1 Bipolar membrane electro-dialysis (BMED) cell

In this study, we used a lab-scale BMED cell assembled with a cation-exchange membrane (Neosepta CMX, Tokuyama Co., Japan), a bipolar membrane (Fumasep FBM, Fuma-Tech Co., Japan), and an anion-exchange membrane (Neosepta AMX, Tokuyama Co., Japan) placed in parallel as shown in Fig. 1. The effective area of each membrane was 17.5 cm^2. Polypropylene mesh with a thickness of 0.5 mm was used as spacer in each flow channel. Ruthenium-coated titanium electrodes were used in anode and cathode compartments of the BMED stack. The BMED cell was operated in a galvanostatic mode as controlled by a potentiostat (SP 150, Bio-Logic, France) that also recorded the real-time system voltage. The simulated wastewater and seawater flowed through the base and acid compartments of the BMED system, respectively, as driven by peristaltic pumps. The electrode rinse solution was pumped through both the anode and cathode compartments. Under the applied electric field, water dissociates within the bipolar membrane (BPM) to generate OH^- ions that enter the base compartment and H^+ ions that enter the acid compartment. In consequence, the seawater and wastewater flowing through the corresponding compartments become acidic and alkaline, respectively.

2.2 Struvite precipitation

The recovery of phosphorus from wastewater was achieved *via* the precipitation of struvite ($MgNH_4PO_4{\cdot}6H_2O$) using the basified wastewater exiting the BMED cell. $MgCl_2{\cdot}6H_2O$ (analytical grade, Sigma-Aldrich, USA) was added into the precipitator as the Mg source. The struvite precipitation was carried out in a continuously stirred tank reactor at room temperature (22 ± 1 °C).

2.3 Multi-stage membrane capacitive deionization (MCDI) system

The multi-stage MCDI system consists of three identical MCDI stacks. Each MCDI stack has a single-pass flow configuration and is operated using constant (CC) charging

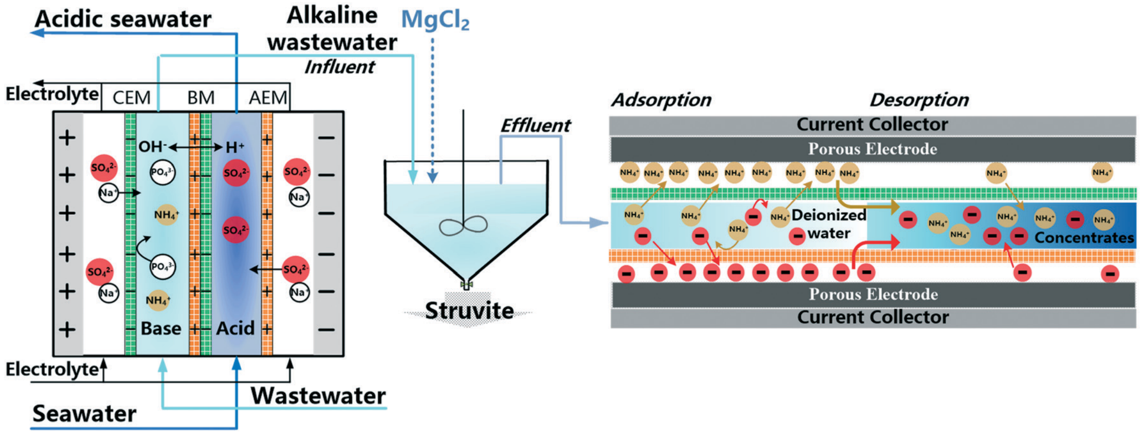

Fig. 1 Schematic diagram of a lab-scale integrated system for simultaneous removal and recovery of phosphorus and ammonium in wastewater. The BMED process increases the pH value of wastewater in the base compartment while acidic seawater is generated in the acid compartment which decreases the solution pH. The alkaline wastewater enters a precipitation reactor for the production of struvite. The effluent from such a reactor, still rich in NH_4^+–N, is further treated by a multi-stage MCDI process for NH_4^+–N recovery.

and discharge. The configuration of the MCDI stacks has been described in detail in previous studies,[27,31] and is also given in the ESI.† Briefly, four MCDI assemblies in parallel were housed in an acrylic housing. Each assembly consists of two film electrodes cast with activated carbon particles (PACMM 203, Materials & Methods LLC, Irvine, CA), an AEM, a CEM (both AEM and CEM are the same as those used in BMED), and a glass fiber filter with a thickness of 250 μm (Whatman) as the spacer. Each assembly was cut to a 6 cm × 6 cm square with a 1.5 cm × 1.5 cm square hole in the center. The total mass of the four pairs of activated carbon electrodes was 3.06 g. Driven by a peristaltic pump, the feed solution enters through the edge of the stack, flows along the spacer channels, and then exits through the center hole.

2.4 Solution chemistry and experimental procedure

A synthetic wastewater with 2.5 mM PO_4^{3-} and 12.5 mM NH_4^+ was prepared by dissolving inorganic salts of NH_4Cl and $NH_4H_2PO_4$ (analytical grade, Sigma-Aldrich) in MilliQ water. The resulting N : P ratio and concentrations are typical of the supernatant of the secondary sedimentation tank in municipal wastewater treatment plants.[4,32] The model seawater was prepared by adding sea salt (Sigma-Aldrich, USA) to DI water at a concentration of 35 g L^{-1}. The seawater was fed to the acidic chamber to increase the electrical conductivity and reduce the overall cell resistance.

In the BMED experiments, a constant volumetric flow rate of 50 ml min^{-1} was used for all streams. We used a semi-batch mode in which the effluent streams from the BMED cell were circulated back to the respective reservoirs with a volume of 500 mL. The seawater and wastewater in the reservoirs thereby became increasingly acidified and alkaline, respectively, which was monitored by measuring the pH in the reservoirs using a pH meter (XL20, Fisher Scientific). The electrode rinse solution (0.1 M Na_2SO_4, 5 L) was circulated through both anode and cathode compartments with a flow rate of 150 mL min^{-1}. The experiments were performed at constant current density (10 to 30 mA cm^{-2}). For each current density, BMED experiments were performed until the target pH for the alkaline wastewater was achieved, and the corresponding operating time and energy consumption (kW h m^{-3}) were calculated.

Once the pH of the wastewater was raised to the target value, the alkaline wastewater was transferred to a precipitator for struvite precipitation to occur for 8 h. A semi-batch mode was used in our experiments because of the relatively small size of the BMED cell. In a real system with a relatively large BMED cell, a single-pass operation mode could be used instead of a semi-batch with recirculation.

The supernatant of the precipitation tank was sampled at various time points for composition measurement. The orthophosphate (PO_4^{3-}–P) and nitrogen (NH_4^+–N) concentrations were determined using ion chromatography (ICS-2100 IC system, Dionex, CA, USA) and a titrimetric method following standard methods (American Public Health Association, 2012), respectively. The precipitate obtained was washed with ultrapure water and dried in an oven at 40 °C for 48 h. The dried precipitate was characterized using X-ray diffraction (XRD) (Rigaku Smart Lab, Japan) and the obtained spectrum was compared with the standard XRD spectrum for the struvite crystal.

The effluent from the struvite precipitator was sent to a multi-stage MCDI system for recovery of NH_4^+–N. In each MCDI cell, the effluent stream in the charging stage (when ions are stored in AC electrodes) is called the deionized water stream, while the effluent stream in the discharge stage (when ions are released to the solution from the AC electrodes) is called the brine stream. In the multi-stage MCDI experiments, the brine stream of the first stage was sent to the next stage as the influent. The deionized water stream from the second MCDI stack was sent to the third MCDI stack as the influent.

The NH_4^+–N concentration of the effluent streams of the MCDI stacks was continuously measured using an ammonium probe. In each stage, the flow rate was controlled to be 3.5 ml min^{-1}, which corresponds to a hydraulic retention time (HRT) of 0.96 min. The MCDI experiments were performed with an operation mode of constant current charging and reverse current discharge (CC-RC) as controlled by a potentiostat (SP 150, Bio-Logic, France) that also recorded the real-time cell voltage. In this study, we choose to use different current densities for charging and discharging, both within one stage and between different stages, with the goal of maximizing NH_4^+–N removal and achieving water recovery, WR.

2.5 Data analysis

The following performance metrics were used to evaluate the performance of the unit processes and the overall sequence. The first performance metric is the specific energy consumption, SEC_{BMED} (kW h m^{-3}), of the BMED process, defined as the energy consumed to produce a unit volume of the alkaline water. The following expression is used to calculate SEC_{BMED}:

$$SEC_{BMED} = \frac{\int_0^t U(t) I A_{BM} dt}{V_a} \tag{1}$$

where $U(t)$ is the voltage of the BMED cell which is dependent on the charging time, t, I is the applied current density, A_{BM} is the effective area of each bipolar membrane, and V_a is the volume of the alkaline solution produced.

In the multi-stage MCDI system, the average effluent and brine NH_4^+–N concentrations for the charging and discharging step in each MCDI stage were calculated based on the following expression:

$$\bar{c} = \frac{\int_0^{t^*} c(t) dt}{t^*} \tag{2}$$

where $c(t)$ is the NH_4^+–N concentration at time t, and t^* is the duration of the charging or discharge step. Water recovery, WR, is defined as the ratio of the volume of the treated water (or diluted water) to the volume of the feed water in each MCDI stage, given by

$$WR = \frac{V_d}{V_d + V_b} \tag{3}$$

where V_d is the volume of the treated water (or diluted water) generated in the charging step and V_b is the volume of the concentrate (or brine solution) produced in the discharge step.

The energy consumption of the MCDI process is quantified as the energy consumed to transfer one mole of NH_4^+–N from the treated water to the concentrate:

$$SEC_N = \frac{\int_0^t U(t) I A_{IEM} dt}{Q \int_0^t (c_0 - c(t)) dt} \tag{4}$$

where I is the applied current density to the MCDI cell, U is the time-dependent cell voltage response, A_{IEM} is the area of each ion exchange membrane which is also the apparent area of the AC electrode, Q is the flow rate of the MCDI stack, and c_0 is the ammonium concentration in the feed stream.

3. Results and discussion

3.1 Alkalinization of wastewater by BMED

The pH of wastewater increased with time in the BMED process because of the continuous generation of OH^- *via* water electrolysis in the bipolar membrane (Fig. 2A). Naturally, a faster increase of pH in the wastewater results from a higher current density that leads to a higher production rate of OH^-. To reach the ideal range of pH for struvite precipitation, which is between 8.5 and 9.0, the BMED process was performed for 20, 10 and 6 min when the current density was 10, 20 and 30 mA cm^{-2}, respectively. Meanwhile, the pH of the seawater stream dropped to 2.2 ± 0.1 in all cases when the ideal pH range for wastewater was reached. Even though both streams have the same flow rate, the change of pH for the seawater stream was more significant than that for the wastewater stream. The buffering capacity against acidification (*i.e.* alkalinity) for seawater was lower than the buffering capacity (from PO_4^{3-} and NH_4^+) against alkalinization of wastewater.

Regardless of the current density, a cell voltage drop was observed in the course of the constant current BMED process due to the reduced resistances for both the seawater and wastewater channels (Fig. 2B). The voltage drop was most significant at the beginning of the BMED process but later leveled off as the acid and base compartments became more concentrated. Such a trend can be explained by the fact that the compartment resistance is inversely proportional to the electrolyte concentration and therefore the increase of

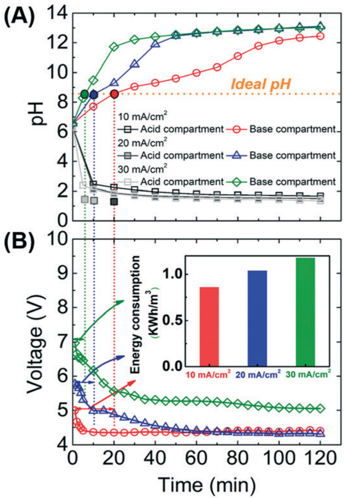

Fig. 2 The changes of pH in acid and base compartments (A) and the change of voltage of the BMED cell (B) as a function of time under different current densities. The inset shows the specific energy consumption of BMED to adjust the pH to 8.55 ± 0.05.

electrolyte concentration has the strongest impact on resistance in the range of low electrolyte concentration.

The specific energy consumption of BMED for achieving the target pH of 8.55 ± 0.05 in the wastewater increases with current density (Fig. 2B inset). There are two major contributions to the energy consumption. First, the process of water electrolysis to generate H^+ and OH^- intrinsically requires minimum energy that corresponds to the Gibbs free energy of the electrochemical conversion. Second, extra energy needs to be provided to drive the process in a finite kinetic rate that is proportional to the current density. For achieving the same pH change of the feed water, the same amount of H^+ and OH^- was generated and thus the same amount of Gibbs free energy was consumed. However, splitting water at a faster rate requires imposing a higher overpotential to provide a larger driving force, which contributes to the difference in SEC at different current densities. In other words, there exists an intrinsic trade-off between energy efficiency and kinetic rate, that is, faster alkalinization of the wastewater would inevitably consume more energy.

3.2 Struvite precipitation in the wastewater effluent from BMED

As shown in Fig. 1, the main purpose of the integrated system is to remove phosphorus and ammonium simultaneously from the wastewater and recover them as nutrients. Phosphorus was recovered from the alkaline wastewater effluent from the BMED cell *via* the formation of struvite which precipitates from Mg^{2+}, NH_4^+, and PO_4^{3-}. Both NH_4^+ and PO_4^{3-} already exist in wastewater and the former is typically overabundant as compared to the stoichiometric ratio of struvite. We therefore added Mg^{2+} into the BMED effluent in a 1 : 1 molar ratio for $Mg^{2+} : PO_4^{3-}$ to initiate the formation of struvite.

As a consequence of struvite precipitation, the PO_4^{3-}–P and NH_4^+–N concentrations of the supernatant decreased over time (Fig. 3A). The concentration profiles of PO_4^{3-}–P and NH_4^+–N suggest that the precipitation proceeded to near complication in only 60 min, which is in accordance with the optimal precipitation time for struvite reported by Xu *et al.*[12] There was about 10% of the ammonium in the influent to the hybrid treatment train that could not be measured in either the precipitate or the solution, which is likely due to evaporation of NH_3 as reported in ref. 33. The phosphate concentration decreased from 2.5 to 0.27 mM, resulting in a phosphate removal efficiency of 89.2%. At the same time, the pH value of the supernatant dropped from 8.55 ± 0.05 to 8.2 ± 0.1 due to struvite formation. XRD analysis of the composition of the formed precipitate reveals major peaks that are consistent with the reference pure struvite crystal standard (Fig. 3B).

3.3 Removal and enrichment of ammonium using multi-stage MCDI

Due to the stoichiometric over-abundance of NH_4^+–N as compared to PO_4^{3-}–P, 72% of NH_4^+–N remained in the supernatant upon the completion of the struvite precipitation (Fig. 3A). To further reduce the effluent NH_4^+–N concentration to meet the discharge standard and to recover NH_4^+–N as a valuable nutrient, we used a multi-stage MCDI process to obtain a solution with enriched NH_4^+–N. Extensive experiments with a variety of operating conditions (*e.g.* the current and flow rate of the charging and discharge stages) have been conducted to optimize this multi-stage MCDI process, with results only from the optimal operating conditions presented in the following discussion.

The three-stage MCDI process was operated as follows: the supernatant from the struvite precipitator, rich in NH_4^+–N, was fed to the first stage MCDI as the feed water (Fig. 4A). In this first stage, the water recovery was 70% and the NH_4^+–N concentration of the treated effluent was ~2.5 mM (Fig. 4B). The brine of the first stage was then sent to the second stage which recovered 55% of the second stage influent (*i.e.*, 16.5% of the overall influent). The average NH_4^+–N concentration of the treated effluent in the second stage was ~15.6 mM, which was still too high for direct discharge. Therefore, the treated effluent in the second stage MCDI was further subjected to a third stage MCDI separation. The water recovery of the third stage MCDI process was 68%, which was

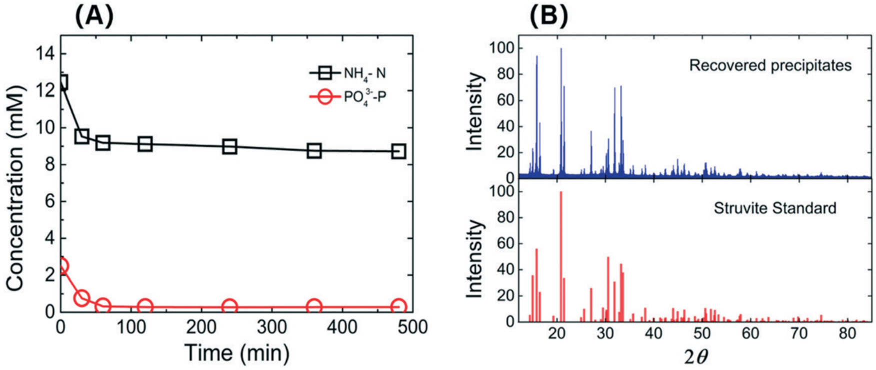

Fig. 3 (A) Concentrations of PO_4^{3-}–P and NH_4^+–N decreased as struvite formed in the precipitator. (B) Powder XRD pattern of the precipitate extracted from the alkaline wastewater in comparison with the standard struvite XRD pattern.

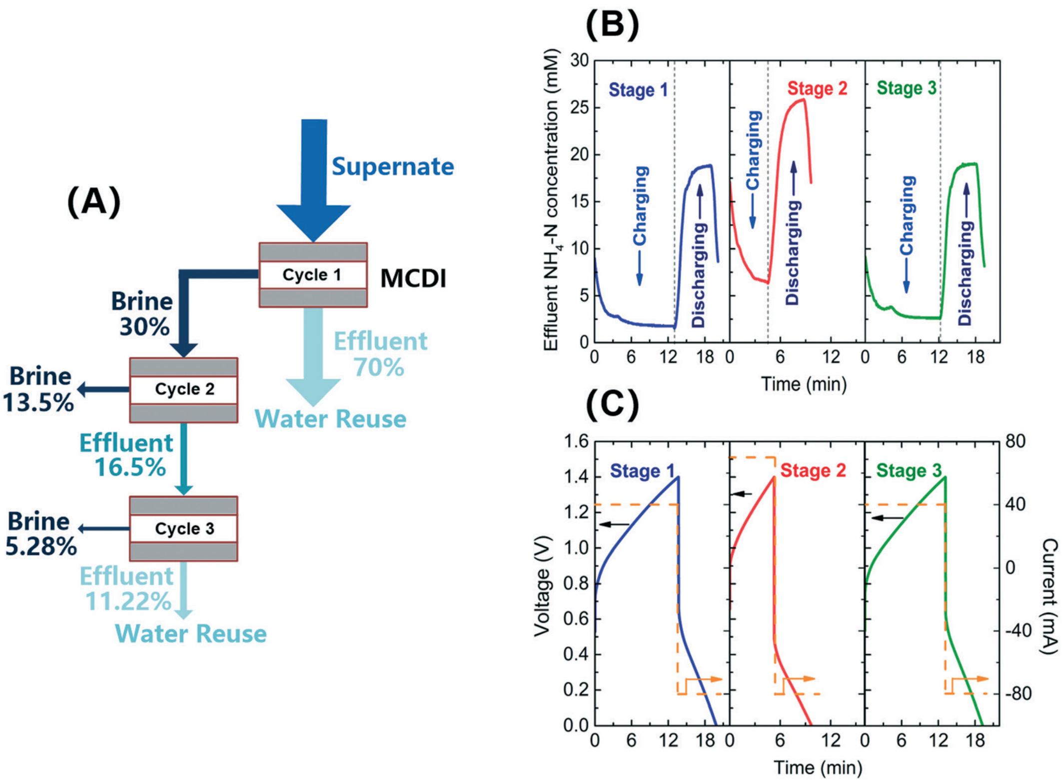

Fig. 4 (A) A schematic diagram of a three-stage MCDI process in which the concentrated brine from the first stage is sent as the feed stream to a two-stage MCDI process for further extraction of ammonia nitrogen. This three-stage process enables a high WR with the effluent of low NH_4^+–N concentration. (B) Cell current and voltage, and (C) effluent NH_4^+–N concentration as a function of time in the charging and discharge steps at different stages. The water flow rate is 3.5 mL min^{-1}.

~11.2% of the influent to the multi-stage MCDI system. The average NH_4^+–N concentration of the treated effluent in the third stage was ~4.6 mM.

In each stage, the MCDI cell was operated using constant current charging and reverse current discharge (*i.e.* a CC-RC mode). The charging current was 40 mA in the first and third stage, and was 70 mA in the second stage due to the higher influent concentration of NH_4^+–N. The discharge current was 80 mA in all stages (Fig. 4C). The flow rate was maintained at 3.5 mL min^{-1} for both charging and discharging in all stages. We chose to terminate charging when the cell voltage reached 1.4 V (to prevent electrolysis of water) and to terminate discharging when the cell voltage reached zero. With this specific operation criterion, the charge–discharge cycle was shorter in the second stage with a higher charging current. Specifically, the full charge–discharge cycle for the second stage is about half that for the first and third stages.

If we define removal efficiency as the percentage reduction of the feed concentration (in the product water) and the enrichment efficiency as the ratio between the brine concentration and feed concentration, the first and third stage MCDI achieved an NH_4^+–N removal efficiency of 72% and an enrichment factor of ~1.9, whereas the second stage MCDI achieved an NH_4^+–N removal efficiency of ~47% and an enrichment efficiency of ~1.4. Overall, the three-stage MCDI process recovered over 81.2% of the effluent of the struvite precipitator with an NH_4^+–N removal efficiency of 72%. It also generated ~18.8% of concentrated NH_4^+–N solution with an overall enrichment factor of ~1.8.

The NH_4^+–N distribution throughout the treatment train and the performance metrics for each MCDI stage are summarized in Fig. 5. The majority (72%) of the NH_4^+–N remained in the effluent of the struvite precipitator, and 18% of the NH_4^+–N was removed from the formed struvite. There was about 10% of NH_4^+–N in the influent to the hybrid treatment train that could not be measured in either the precipitate or the solution, which is likely due to the evaporation of NH_3 as reported in the literature.[33] The NH_4^+–N accounting suggests that the first stage MCDI process alone could remove 72% of the NH_4^+–N in the influent stream and recover 70% of water. Notably, the first stage MCDI process also consumed the least energy (1.87 kW h kg^{-1} N).

However, further enhancing water recovery becomes increasingly difficult. The second and third stages combined only recovered ~12% more water while consuming much more energy for NH_4^+–N removal. Specifically, the second and third stages consumed 2.80 and 2.11 kW h kg^{-1} N, respectively. With the tested flow rate and the same level of NH_4^+–N removal, the total treatment time for achieving 82% water recovery was 49 min, which is nearly two and half times longer than achieving a water recovery of 70%. Therefore, there is a diminishing return in both the aspects

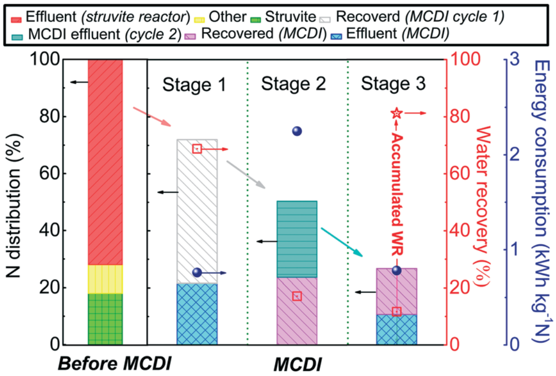

Fig. 5 Distribution of NH_4^+–N (bar), water recovery (red square), and specific energy consumption (blue circle) in the electrochemical sequence. The hybrid process recovers 82% water, removes ~100% PO_4^{3-}–P in the form of struvite and 77% of NH_4^+–N in the form of both struvite and NH_4^+–N concentrate.

of energy consumption and kinetics when the MCDI system was challenged to achieve a higher water recovery.

The overall process of MCDI was to generate two diluted streams and two brine streams. The energy requirement of the three-stage MCDI system was 3.22 kW h kg^{-1} N that is consumed to concentrate N from the precipitation supernatant (feed) to the brine of the MCDI system, which is very competitive with other NH_4^+–N removal/recovery technologies. For instance, the energy requirement for NH_4^+–N removal by the conventional activated sludge process (based on nitrification and denitrification) ranges from 6.18–13.6 kW h kg^{-1} N.[34] When microbial and electrochemical processes are combined, namely a bio-electrochemical system (BES) and BES-based system with the representative examples as a microbial fuel cell and microbial electrolysis cell, ammonia may be removed and recovered with a much lower energy consumption.[35–37] However, biological processes still require long start-up times and are sensitive to environmental factors (*e.g.* pH, temperature and influent quality).[38] The three-stage MCDI process reported in this study also consumed less energy when compared with FCDI or FCDI-based processes that have been reported to consume 6.1–21.7 kW h kg^{-1} N.[33,39]

4. Conclusions

We have demonstrated an integrated system that incorporates BMED, a struvite reactor and multi-stage MCDI in sequence. This system with two major electrochemical components, BMED and MCDI, enables efficient removal and recovery (enrichment) of nutrients from wastewater with minimal use of chemicals. While the economic competitiveness of BMED as compared to chemical dosing for pH adjustment requires more extensive techno-economic analysis, BMED as an alternative for pH adjustment converts the chemical consumption to energy consumption and thus can potentially be powered by sustainable energy. The prevention of using chemicals for pH adjustment is also beneficial to the subsequent removal of NH_4^+, because it reduces the amount of counter ions (cations in this case) in the feed water entering the MCDI system, which reduces the competitive adsorption of other cations *vs.* NH_4^+ and thereby reduces energy consumption for NH_4^+ recovery.

The proposed electro-chemical sequence also has high adaptability to different source waters and target water quality. While we use treated wastewater as an example in this study, the electro-chemical sequence may also be used for efficient removal and recovery (enrichment) of nutrients from feed streams of high nutrient concentrations and large N/P ratios (>10, *e.g.* urine and pig manure). The two major operating parameters, including applied current density and hydraulic residence time, can be tuned simultaneously to achieve the target treatment goal.

Conflicts of interest

There is no conflict to declare.

Acknowledgements

F. G. acknowledges the support from the China Scholarship Council (201806250113). L. W. and S. L. acknowledge the support from the Natural Science Foundation *via* research grant 1739884.

References

1 P. Falkowski, R. J. Scholes, E. Boyle, J. Canadell, D. Canfield, J. Elser, N. Gruber, K. Hibbard, P. Hogberg, S. Linder, F. T. Mackenzie, B. Moore, T. Pedersen, Y. Rosenthal, S. Seitzinger, V. Smetacek and W. Steffen, The global carbon cycle: A test of our knowledge of earth as a system, *Science*, 2000, **290**, 291–296.
2 D. Cordell, A. Rosemarin, J. J. Schroder and A. L. Smit, Towards global phosphorus security: A systems framework for phosphorus recovery and reuse options, *Chemosphere*, 2011, **84**, 747–758.
3 Y. Zhang, E. Desmidt, A. Van Looveren, L. Pinoy, B. Meesschaert and B. Van der Bruggen, Phosphate Separation and Recovery from Wastewater by Novel Electrodialysis, *Environ. Sci. Technol.*, 2013, **47**, 5888–5895.
4 S. H. Lee, B. H. Yoo, S. K. Kim, S. J. Lim, J. Y. Kim and T. H. Kim, Enhancement of struvite purity by re-dissolution of calcium ions in synthetic wastewaters, *J. Hazard. Mater.*, 2013, **261**, 29–37.
5 J. Driver, D. Lijmbach and I. Steen, Why recover phosphorus for recycling, and how?, *Environ. Technol.*, 1999, **20**, 651–662.
6 R. D. Schuiling and A. Andrade, Recovery of struvite from calf manure, *Environ. Technol.*, 1999, **20**, 765–768.
7 D. J. Conley, H. W. Paerl, R. W. Howarth, D. F. Boesch, S. P. Seitzinger, K. E. Havens, C. Lancelot and G. E. Likens, Controlling Eutrophication: Nitrogen and Phosphorus, *Science*, 2009, **323**, 1014.
8 S. Agrawal, J. S. Guest and R. D. Cusick, Elucidating the impacts of initial supersaturation and seed crystal loading

on struvite precipitation kinetics, fines production, and crystal growth, *Water Res.*, 2018, **132**, 252–259.

9 J. Jack, T. M. Huggins, Y. P. Huang, Y. F. Fang and Z. J. Ren, Production of magnetic biochar from waste-derived fungal biomass for phosphorus removal and recovery, *J. Cleaner Prod.*, 2019, **224**, 100–106.

10 N. Zhao, H. Wang, Z. He and Q. Yan, Ammonia removal and recovery from diluted forward osmosis draw solution by using a tubular microbial desalination cell, *Environ. Sci.: Water Res. Technol.*, 2019, **5**, 224–230.

11 M. H. Qin, E. A. Hynes, I. M. Abu-Reesh and Z. He, Ammonium removal from synthetic wastewater promoted by current generation and water flux in an osmotic microbial fuel cell, *J. Cleaner Prod.*, 2017, **149**, 856–862.

12 K. N. Xu, J. Y. Li, M. Zheng, C. Zhang, T. Xie and C. W. Wang, The precipitation of magnesium potassium phosphate hexahydrate for P and K recovery from synthetic urine, *Water Res.*, 2015, **80**, 71–79.

13 L. T. Angenent, K. Karim, M. H. Al-Dahhan and R. Domiguez-Espinosa, Production of bioenergy and biochemicals from industrial and agricultural wastewater, *Trends Biotechnol.*, 2004, **22**, 477–485.

14 J. D. Doyle and S. A. Parsons, Struvite formation, control and recovery, *Water Res.*, 2002, **36**, 3925–3940.

15 Y. H. Song, G. L. Qiu, P. Yuan, X. Y. Cui, J. F. Peng, P. Zeng, L. Duan, L. C. Xiang and F. Qian, Nutrients removal and recovery from anaerobically digested swine wastewater by struvite crystallization without chemical additions, *J. Hazard. Mater.*, 2011, **190**, 140–149.

16 A. Adnan, M. Dastur, D. S. Mavinic and F. A. Koch, Preliminary investigation into factors affecting controlled struvite crystallization at the bench scale, *J. Environ. Eng. Sci.*, 2004, **3**, 195–202.

17 Y. H. Bian, X. Chen, L. Lu, P. Liang and Z. J. Ren, Concurrent Nitrogen and Phosphorus Recovery Using Flow-Electrode Capacitive Deionization, *ACS Sustainable Chem. Eng.*, 2019, **7**, 7844–7850.

18 Y. C. Chiao, F. P. Chlanda and K. N. Mani, Bipolar Membranes for Purification of Acids and Bases, *J. Membr. Sci.*, 1991, **61**, 239–252.

19 S. Mafe, P. Ramirez and A. Alcaraz, Electric field-assisted proton transfer and water dissociation at the junction of a fixed-charge bipolar membrane, *Chem. Phys. Lett.*, 1998, **294**, 406–412.

20 Y. Y. Chen, J. R. Davis, C. H. Nguyen, J. C. Baygents and J. Farrell, Electrochemical Ion-Exchange Regeneration and Fluidized Bed Crystallization for Zero-Liquid-Discharge Water Softening, *Environ. Sci. Technol.*, 2016, **50**, 5900–5907.

21 L. Shi, Y. S. Hu, S. H. Xie, G. X. Wu, Z. H. Hu and X. M. Zhan, Recovery of nutrients and volatile fatty acids from pig manure hydrolysate using two-stage bipolar membrane electrodialysis, *Chem. Eng. J.*, 2018, **334**, 134–142.

22 Y. M. Zhou, H. Y. Yan, X. L. Wang, Y. M. Wang and T. W. Xu, A closed loop production of water insoluble organic acid using bipolar membranes electrodialysis (BMED), *J. Membr. Sci.*, 2016, **520**, 345–353.

23 M. Chen, F. Zhang, Y. Zhang and R. J. Zeng, Alkali production from bipolar membrane electrodialysis powered by microbial fuel cell and application for biogas upgrading, *Appl. Energy*, 2013, **103**, 428–434.

24 S. Mikhaylin, L. Patouillard, M. Margni and L. Bazinet, Milk protein production by a more environmentally sustainable process: bipolar membrane electrodialysis coupled with ultrafiltration, *Green Chem.*, 2018, **20**, 449–456.

25 M. D. Eisaman, K. Parajuly, A. Tuganov, C. Eldershaw, N. R. Chang and K. A. Littau, CO_2 extraction from seawater using bipolar membrane electrodialysis, *Energy Environ. Sci.*, 2012, **5**, 7346–7352.

26 S. Porada, R. Zhao, A. van der Wal, V. Presser and P. M. Biesheuvel, Review on the science and technology of water desalination by capacitive deionization, *Prog. Mater. Sci.*, 2013, **58**, 1388–1442.

27 L. Wang and S. H. Lin, Membrane Capacitive Deionization with Constant Current vs Constant Voltage Charging: Which Is Better?, *Environ. Sci. Technol.*, 2018, **52**, 4051–4060.

28 L. Wang and S. H. Lin, Theoretical framework for designing a desalination plant based on membrane capacitive deionization, *Water Res.*, 2019, **158**, 359–369.

29 Z. Ge, X. Chen, X. Huang and Z. Y. J. S. Ren, Capacitive deionization for nutrient recovery from wastewater with disinfection capability, *Environ. Sci.: Water Res. Technol.*, 2018, **4**, 33–39.

30 S. I. Jeon, H. R. Park, J. G. Yeo, S. Yang, C. H. Cho, M. H. Han and D. K. Kim, Desalination via a new membrane capacitive deionization process utilizing flow-electrodes, *Energy Environ. Sci.*, 2013, **6**, 1471–1475.

31 L. Wang and S. H. Lin, Mechanism of Selective Ion Removal in Membrane Capacitive Deionization for Water Softening, *Environ. Sci. Technol.*, 2019, **53**, 5797–5804.

32 A. J. Ward, K. Arola, E. T. Brewster, C. M. Mehta and D. J. Batstone, Nutrient recovery from wastewater through pilot scale electrodialysis, *Water Res.*, 2018, **135**, 57–65.

33 C. Y. Zhang, J. X. Ma, D. He and T. D. Waite, Capacitive Membrane Stripping for Ammonia Recovery (CapAmm) from Dilute Wastewaters, *Environ. Sci. Technol. Lett.*, 2018, **5**, 43–49.

34 M. Maurer, P. Schwegler and T. A. Larsen, Nutrients in urine: energetic aspects of removal and recovery, *Water Sci. Technol.*, 2003, **48**, 37–46.

35 P. Kuntke, K. M. Smiech, H. Bruning, G. Zeeman, M. Saakes, T. H. J. A. Sleutels, H. V. M. Hamelers and C. J. N. Buisman, Ammonium recovery and energy production from urine by a microbial fuel cell, *Water Res.*, 2012, **46**, 2627–2636.

36 Y. F. Zhang and I. Angelidaki, Recovery of ammonia and sulfate from waste streams and bioenergy production via bipolar bioelectrodialysis, *Water Res.*, 2015, **85**, 177–184.

37 P. Zamora, T. Georgieva, A. Ter Heijne, T. H. J. A. Sleutels, A. W. Jeremiasse, M. Saakes, C. J. N. Buisman and P. Kuntke, Ammonia recovery from urine in a scaled-up Microbial Electrolysis Cell, *J. Power Sources*, 2017, **356**, 491–499.

38 Y. F. Zhang and I. Angelidaki, Submersible microbial desalination cell for simultaneous ammonia recovery and electricity production from anaerobic reactors containing high levels of ammonia, *Bioresour. Technol.*, 2015, **177**, 233–239.

39 C. Y. Zhang, J. X. Ma, J. K. Song, C. He and T. D. Waite, Continuous Ammonia Recovery from Wastewaters Using an Integrated Capacitive Flow Electrode Membrane Stripping System, *Environ. Sci. Technol.*, 2018, **52**, 14275–14285.